A Patch-Structure Representation Method for Quality Assessment of Contrast Changed Images

Shiqi Wang, *Member, IEEE*, Kede Ma, *Student Member, IEEE*, Hojatollah Yeganeh, *Member, IEEE*, Zhou Wang, *Fellow, IEEE*, and Weisi Lin, *Senior Member, IEEE*

***Abstract*—Contrast is a fundamental attribute of images that plays an important role in human visual perception of image quality. With numerous approaches proposed to enhance image contrast, much less work has been dedicated to automatic quality assessment of contrast changed images. Existing approaches rely on global statistics to estimate contrast quality. Here we propose a novel local patch-based objective quality assessment method using an adaptive representation of local patch structure, which allows us to decompose any image patch into its mean intensity, signal strength and signal structure components and then evaluate their perceptual distortions in different ways. A unique feature that differentiates the proposed method from previous contrast quality models is the capability to produce a local contrast quality map, which predicts local quality variations over space and may be employed to guide contrast enhancement algorithms. Validations based on four publicly available databases show that the proposed patch-based contrast quality index (PCQI) method provides accurate predictions on the human perception of contrast variations.**

***Index Terms*—Contrast change, image quality assessment, patch representation, structural information.**

I. Introduction

CONTRAST is a fundamental perceptual attribute of images that makes the representation of objects distinguishable [1]. In many applications, contrast is a determining factor in human perception of image quality. During image acquisition, the limitations of acquisition devices, together with imperfect lighting conditions, may result in low contrast images. This has inspired numerous contrast enhancement techniques [2]. However, such enhancement methods are often demonstrated and compared qualitatively by specific examples, without quantitative evaluations by trusted image quality assessment (IQA) models. Therefore, objective IQA models that can predict the perceptual quality of contrast changed images is desirable, which also provide essential guidance in devising and optimizing advanced contrast enhancement algorithms. However, this is a non-trivial problem that has not been well resolved. Traditional full-reference (FR) IQA often makes a strong assumption that the reference image has perfect quality, which does not hold in IQA of contrast changed images, where the processed images may have even better perceptual appearance. Most existing methods judge the contrast quality from global statistics such as the entropy, sample mean and standard deviation of pixel intensities [3]–[5]. In [3], a no-reference (NR) IQA method for contrast enhancement was proposed based on the principle of natural scene statistics (NSS). In [4], a reduced-reference (RR) method was proposed based on moment statistics. In [5], the contrast quality is determined by the histogram flatness and spread.

In this work, instead of relying on global statistics, we propose a patch-based approach. Specifically, we represent any image patch in a unique and adaptive way as three conceptually independent components: mean intensity, signal strength and signal structure. The motivation behind this decomposition is that even though the original image may not have perfect contrast, it is considered the faithful source that contains the structural information, and thus it is desirable to separate structure representation from mean intensity and signal strength, so that their distortions can be measured separately. The proposed method not only predicts the overall contrast quality of the test image, but also produces a quality map that indicates local quality variations over space.

II. IQA of Contrast Changed Images

Given a $\sqrt{N} \times \sqrt{N}$ local image patch $\mathbf{x}$ that is represented as an N-dimensional vector, we decompose it by

$$\begin{aligned}\mathbf{x} &= \mu_{\mathbf{x}} + \|\mathbf{x} - \mu_{\mathbf{x}}\| \cdot \frac{\mathbf{x} - \mu_{\mathbf{x}}}{\|\mathbf{x} - \mu_{\mathbf{x}}\|} \\ &= c_1^{\mathbf{x}} \cdot \mathbf{v}_1 + c_2^{\mathbf{x}} \cdot \mathbf{v}_2, \end{aligned} \tag{1}$$

where $\|\cdot\|$ denotes the l^2 norm of a vector and $\mu_{\mathbf{x}}$ is the mean intensity of the local patch. $\mathbf{x}$ is now represented as a linear combination of two unit-length vectors,

$$\mathbf{v}_1 = \frac{1}{\sqrt{N}} \cdot \mathbf{1}, \quad \mathbf{v}_2 = \frac{\mathbf{x} - \mu_{\mathbf{x}}}{\|\mathbf{x} - \mu_{\mathbf{x}}\|}, \tag{2}$$

each associated with a coefficient

$$c_1^{\mathbf{x}} = \sqrt{N}\mu_{\mathbf{x}}, \quad c_2^{\mathbf{x}} = \|\mathbf{x} - \mu_{\mathbf{x}}\|. \tag{3}$$

Here $\mathbf{1}$ denotes a column vector with all entries equaling 1. Since $\mathbf{v}_1$ is fixed, each source patch $\mathbf{x}$ can be uniquely represented by three components $c_1^{\mathbf{x}}$, $c_2^{\mathbf{x}}$ and the unit-length vector

Manuscript received July 01, 2015; revised August 22, 2015; accepted September 24, 2015. Date of publication October 05, 2015; date of current version October 09, 2015. The associate editor coordinating the review of this manuscript and approving it for publication was Prof. Guy Gilboa.

S. Wang, K. Ma, H. Yeganeh, and Z. Wang are with the Department of Electrical and Computer Engineering, University of Waterloo, Waterloo, ON N2L 3G1 Canada (e-mail: s269wang@uwaterloo.ca; k29ma@uwaterloo.ca; hyeganeh@uwaterloo.ca; zhou.wang@uwaterloo.ca).

W. Lin is with the School of Computer Engineering, Nanyang Technological University, Singapore (e-mail: wslin@ntu.edu.sg).

Color versions of one or more of the figures in this paper are available online at http://ieeexplore.ieee.org.

Digital Object Identifier 10.1109/LSP.2015.2487369

1070-9908 © 2015 IEEE. Personal use is permitted, but republication/redistribution requires IEEE permission.
See http://www.ieee.org/publications_standards/publications/rights/index.html for more information.

Authorized licensed use limited to: Access paid by The UC Irvine Libraries. Downloaded on March 24,2021 at 13:49:33 UTC from IEEE Xplore. Restrictions apply.

Fig. 1. Example of contrast stretched/compressed images along the direction of the structure vector $\mathbf{v}_2$.

$\mathbf{v}_2$, which represent the mean intensity, signal strength and signal structure, respectively. Such a representation or decomposition is adaptive, where the basis $\mathbf{v}_2$ points to a specific direction in the signal space and is adapted to the input signal. This representation also gives us a new coordinate system in the image patch space, where any new patch $\mathbf{y}$ can be written as

$$\mathbf{y} = c_1^{\mathbf{y}} \cdot \mathbf{v}_1 + c_2^{\mathbf{y}} \cdot \mathbf{v}_2 + \mathbf{r}, \tag{4}$$

where

$$\begin{aligned} c_1^{\mathbf{y}} &= \mathbf{y}^T \mathbf{v}_1 = \sqrt{N}\mu_{\mathbf{y}} \\ c_2^{\mathbf{y}} &= \mathbf{y}^T \mathbf{v}_2, \end{aligned} \tag{5}$$

and $\mathbf{r}$ is the residual signal perpendicular to both $\mathbf{v}_1$ and $\mathbf{v}_2$.

Now assume $\mathbf{x}$ and $\mathbf{y}$ are a pair of co-located patches in the original image $\mathbf{X}$ and test image $\mathbf{Y}$, respectively. Based on the philosophy that the human visual perception is highly adapted for extracting structural information from a natural scene [6], the contrast change is characterized by the scaling of the signal strength along the direction of $\mathbf{v}_2$. Specifically, we define

$$q_c(\mathbf{x}, \mathbf{y}) = \frac{4}{\pi} \cdot \arctan\left(\left| \frac{c_2^{\mathbf{y}}}{c_2^{\mathbf{x}}} \right| \right), \tag{6}$$

where the nonlinear function $\frac{4}{\pi} \cdot \arctan(\cdot)$ is introduced to control the saturation of the contrast change, so that $q_c(\mathbf{x}, \mathbf{y})$ is bounded between 0 and 2.

In comparison with the reference image, a better contrast image results in a q_c score larger than unity. Fig. 1 shows examples of signal contrast changed images, where the images are created by stretching or compressing $c_2^{\mathbf{x}}$ along $\mathbf{v}_2$ direction while maintaining $\mathbf{r} = 0$ and $c_1^{\mathbf{x}} = c_1^{\mathbf{y}}$. It is easy to observe that by strengthening $c_2^{\mathbf{x}}$, better contrast images are obtained, corresponding to quality scores greater than unity. By contrast, shrinking $c_2^{\mathbf{x}}$ lowers the contrast and subsequently degrades the image quality.

The present framework implies that when the residual vector $\mathbf{r} = 0$, there is no structural distortions. In other words, the structural distortion is determined by the relative strength of $\mathbf{r}$, especially how it leads the test signal structure to depart from $\mathbf{v}_2$. To capture this, we define

$$q_s(\mathbf{x}, \mathbf{y}) = \cos \angle(\mathbf{v}_2, c_2^{\mathbf{y}} \cdot \mathbf{v}_2 + \mathbf{r}) = \frac{c_2^{\mathbf{y}} + \mathbf{r}^T \mathbf{v}_2}{\| c_2^{\mathbf{y}} \cdot \mathbf{v}_2 + \mathbf{r} \|}, \tag{7}$$

where $\angle(\cdot, \cdot)$ denotes the angle between two vectors.

As such, the difference between $\mathbf{x}$ and $\mathbf{y}$ are quantified by the variations on signal strength and signal structure, which are in accordance with the philosophy of the signal decomposition in (1).

To compare the mean intensity, we apply an exponential function based on the absolute difference between $c_1^{\mathbf{x}}$ and $c_1^{\mathbf{y}}$,

$$q_i(\mathbf{x}, \mathbf{y}) = e^{\left(-\frac{|c_1^{\mathbf{x}} - c_1^{\mathbf{y}}|}{\sqrt{N} L} \right)}, \tag{8}$$

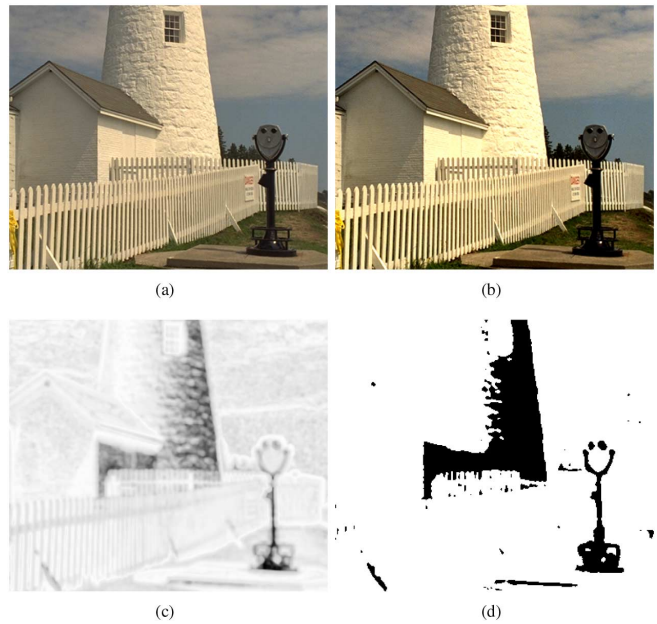

Fig. 2. Contrast enhanced image, and its corresponding PCQI and binary degradation maps. (a) Original image. (b) Contrast enhanced image. (c) PCQI map (brighter indicates higher PCQI value). (d) Local binary quality degradation map (black indicates PCQI < 1).

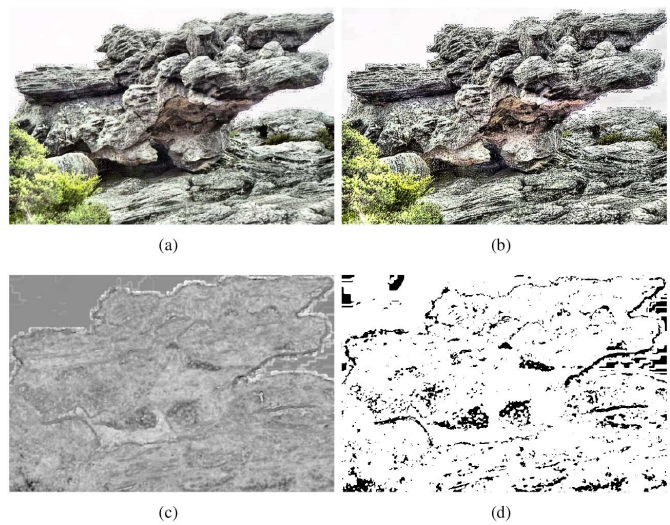

Fig. 3. Contrast enhanced image, and its corresponding PCQI and binary degradation maps. (a) Original image. (b) Contrast enhanced image. (c) PCQI map (brighter indicates higher PCQI value). (d) Local binary quality degradation map (black indicates PCQI < 1).

where L is the dynamic range of the pixel values (255 for 8-bit images).

Finally, the three comparisons as defined in (6), (7) and (8) are combined together, resulting in a patch-based contrast image quality index denoted by PCQI,

$$\mathrm{PCQI}(\mathbf{x}, \mathbf{y}) = q_i(\mathbf{x}, \mathbf{y}) \cdot q_c(\mathbf{x}, \mathbf{y}) \cdot q_s(\mathbf{x}, \mathbf{y}). \tag{9}$$

One significant advantage of PCQI is that when it is applied to local patches across the image, a spatially varying quality map is created, which delivers useful information about the local quality variations across space. Figs. 2 and 3 demonstrate two examples of contrast enhanced images together with their corresponding PCQI maps (where brighter indicates better quality)

Authorized licensed use limited to: Access paid by The UC Irvine Libraries. Downloaded on March 24,2021 at 13:49:33 UTC from IEEE Xplore. Restrictions apply.

TABLE I
SRCC AND PLCC PERFORMANCE EVALUATION BASED ON FOUR IMAGE DATABASES

	TID2008 (200 images)		TID2013 (250 images)		CID2013 (400 images)		CSIQ (116 images)		Weighted Average	
	SRCC	PLCC	SRCC	PLCC	SRCC	PLCC	SRCC	PLCC	SRCC	PLCC
SSIM	0.5193	0.5470	0.4992	0.5735	0.8228	0.8218	0.7922	0.7891	0.6725	0.6967
FSIM	0.4388	0.6878	0.4398	0.6761	0.8486	0.8575	0.9421	0.9435	0.6692	0.7857
GMSD	0.4511	0.6802	0.4451	0.6754	0.8803	0.8818	0.9039	0.9232	0.6816	0.7916
MS-SSIM	0.4641	0.6889	0.4582	0.6846	0.8580	0.8686	0.9526	0.9531	0.6843	0.7939
IW-SSIM	0.4503	0.6996	0.4528	0.6907	0.8632	0.8756	0.9539	**0.9614**	0.6824	0.8016
PSNR	0.5207	0.4750	0.5020	0.5200	0.6649	0.6504	0.8621	0.8888	0.6166	0.6090
VSI	0.4571	0.6865	0.4643	0.6775	0.8504	0.8571	0.9504	0.9533	0.6811	0.7869
GSIM	0.5126	0.6738	0.4985	0.6589	0.8372	0.8353	0.9354	0.9325	0.6941	0.7679
VIF	0.7878	0.8375	0.7716	0.8458	0.8683	0.8771	0.9345	0.9439	0.8346	0.8688
NR-CDIQA	0.5288	0.5703	0.5015	0.6588	0.8874	0.9096	0.8044	0.8508	0.7033	0.7674
RIQMC	0.7316	0.7733	0.7239	0.7848	0.9133	0.9080	**0.9576**	0.9593	0.8320	0.8544
PCQI	**0.8685**	**0.9105**	**0.8787**	**0.9212**	**0.9247**	**0.9236**	0.9499	0.9494	**0.9042**	**0.9234**

and binary maps that indicate the spatial locations where the quality is degraded ($\mathrm{PCQI} < 1$) rather than enhanced. In general the enhanced image in Fig. 2(b) is perceptually more appealing than the original image in Fig. 2(a), but scrupulous observers may find that certain parts of the image are overenhanced (for example the brightest regions of the lighthouse), leading to loss of structural details. It can be seen that the PCQI map in Fig. 2(c) successfully captures such quality degradations. In Fig. 3(b), many fine details in the image are strongly enhanced, but meanwhile some artificial artifacts are created, especially near the edges of the objects. Again, the PCQI map in Fig. 3(c) successfully detects those problematic regions. These examples demonstrate the potentials of using PCQI map to guide the design and optimization of image enhancement algorithms.

The local PCQI for each patch is averaged to provide a single score of the entire image,

$$\mathrm{PCQI}(\mathbf{X}, \mathbf{Y}) = \frac{1}{M} \sum_{j=1}^{M} \mathrm{PCQI}(\mathbf{x}_j, \mathbf{y}_j), \tag{10}$$

where M is the total number of patches. It is worth noting that when $\mathbf{X} = \mathbf{Y}$, PCQI is exactly unity. On the other hand, $\mathrm{PCQI}(\mathbf{X}, \mathbf{Y}) = 1$ does not imply $\mathbf{X} = \mathbf{Y}$. One possible scenario is that the contrast is enhanced while certain structural or mean intensity distortion is also introduced. In such cases, the PCQI value represents a compromise between contrast enhancement and structure/mean intensity distortions.

The general philosophy of PCQI is similar to the structural similarity index (SSIM) [6]. The differences are manifold. First, the proposed patch-based representation explicitly constructs a locally-adaptive coordinate system that allows for decomposing any new signal into three physically meaningful components; Second, unlike SSIM, the strength of the components is obtained by projection in the new coordinate system; Third, unlike the contrast evaluation component in SSIM, the q_c value could be larger than 1 when the signal strength is enhanced.

III. VALIDATION

To validate the performance of the proposed algorithm, four datasets that contain contrast changed images are employed, including CID2013 [4], TID2008 [7], TID2013 [8], and CSIQ [9]. CID2013 is specifically designed for evaluating the quality of contrast changed images, and contains 15 reference and 400 distorted images in total. TID 2008 contains 1700 test images (25 reference images, and 17 types of distortions at 4 different levels), among which 200 images are directly related to contrast distortions (mean shift and contrast change). TID2013 introduces five distortion levels and 250 images are included for testing. CSIQ contains various distortion types, among which there are 116 global contrast changed images.

We compare the proposed method with both classical and state-of-the-art FR quality assessment algorithms, including PSNR, SSIM [6], MS-SSIM [10], IW-SSIM [11], GSIM [12], FSIM [13], GMSD [14], VSI [15] and VIF [16]. Moreover, the NR (NR-CDIQA [3]) and RR (RIQMC [4]) methods that are specifically designed for contrast changed images are included as well. Spearman rank-order correlation coefficient (SRCC) and Pearson linear correlation coefficient (PLCC) results are reported. PLCC evaluates prediction accuracy with a nonlinear mapping between the subjective and objective scores. SRCC is a nonparametric rank-order based correlation metric that is independent of any monotonic score mapping. It is employed to assess prediction monotonicity. A better objective quality is expected to achieve higher values in PLCC and SRCC.

The test results of the four databases are shown in Table I, where the proposed PCQI method clearly outperforms state-of-the-art quality assessment algorithms on TID2008, TID2013 and CID2013 databases, and is among the best for CSIQ database. The average performance over four databases weighted in terms of the number of test images is summarized at the rightmost of Table I, which demonstrates the superior performance of the proposed PCQI method.

Furthermore, we carried out a statistical significant analysis based on a variance-based hypothesis testing following the approach in [17], where the residual difference between the DMOS and the predicted score from the objective IQA algorithm is assumed to follow the Gaussian distribution, and thus F-statistic is employed to compare the variances of two sets of sample points. The statistical significance matrix is given in Table II, in which each entry consists of four characters corresponding to the test databases in the order of TID2008, TID2013, CID2013, and CSIQ, respectively. A symbol "-" denotes that the row and column IQA models are statistically indistinguishable, "1" denotes that the IQA method of the row is statistically better than that of the column, and "0" denotes

Authorized licensed use limited to: Access paid by The UC Irvine Libraries. Downloaded on March 24,2021 at 13:49:33 UTC from IEEE Xplore. Restrictions apply.

TABLE II
STATISTICAL SIGNIFICANCE MATRIX BASED ON IQA-DMOS RESIDUALS

IQA Model	SSIM	FSIM	GMSD	MS-SSIM	IW-SSIM	PSNR	VSI	GSIM	VIF	NR-CDIQA	RIQMC	PCQI
SSIM	----	0-00	--00	1-00	0000	--10	0-00	---0	0000	--00	0000	0000
FSIM	1-11	----	----	1---	---0	1111	----	----	00--	1-01	000-	000-
GMSD	--11	----	----	1--0	---0	111-	---0	--1-	00--	--0-	0000	0000
MS-SSIM	0-11	0---	0--1	----	0---	-111	0---	0-1-	00--	0-01	000-	000-
IW-SSIM	1111	---1	---1	1---	----	1111	----	--11	00--	1-01	000-	000-
PSNR	--01	0000	000-	-000	0000	----	0000	0000	0000	-00-	0000	0000
VSI	1-11	----	---1	1---	----	1111	----	----	00--	1-01	000-	000-
GSIM	---1	----	--0-	1-0-	--00	1111	----	----	000-	--01	000-	000-
VIF	1111	11--	11--	11--	11--	1111	11--	111-	----	1101	110-	000-
NR-CDIQA	--11	0-10	--1-	1-10	0-10	-11-	0-10	--10	0010	----	00-0	0000
RIQMC	1111	111-	1111	111-	111-	1111	111-	111-	001-	11-1	----	000-
PCQI	1111	111-	1111	111-	111-	1111	111-	111-	111-	1111	111-	----

TABLE III
RUNNING TIME OF DIFFERENT IQA METHODS

IQA Methods	SSIM	FSIM	GSMD	MS-SSIM	IW-SSIM	PSNR	VSI	GSIM	VIF	PCQI
Running Time (s)	0.0114	0.1643	0.0047	0.0469	0.2898	0.0009	0.1192	0.0139	0.6704	0.0230

that the IQA method of the column is better than that of the row. It can be observed that the PCQI model is statistically superior to state-of-the-art FR IQA algorithms and other contrast quality models in most cases.

Table III shows the running time of different IQA methods. Specifically, we run ten IQA methods on the TID 2008 database. All algorithms are run on a computer with Intel Core i7-4770 CPU@3.4 GHz and 8G RAM. The software platform used to run all algorithms is MATLAB R2014. The average running time is computed. It can be observed that the computational complexity of the proposed method is among the lowest in state-of-the-art IQA algorithms.

IV. CONCLUSION

We develop an objective model to assess the quality of contrast changed images by introducing a novel adaptive patch representation method. Experimental results show that the proposed PCQI method is well correlated with subjective evaluations of image quality, suggesting that the proposed model is promising at handling contrast changed images. The PCQI map produced by the proposed method also indicates local quality variations, which are useful in guiding the future design of advanced image enhancement algorithms.

REFERENCES

[1] E. Peli, "Contrast in complex images," *J. Opt. Soc. Amer. A*, vol. 7, no. 10, pp. 2032–2040, 1990.

[2] H. K. Sawant and M. Deore, "A comprehensive review of image enhancement techniques," *Int. J. Comput. Technol. Electron. Eng.*, vol. 1, no. 2, 2011.

[3] Y. Fang, K. Ma, Z. Wang, W. Lin, Z. Fang, and G. Zhai, "No-reference quality assessment of contrast-distorted images based on natural scene statistics," *IEEE Signal Process. Lett.*, vol. 22, no. 7, pp. 838–842, 2015.

[4] K. Gu, G. Zhai, X. Yang, W. Zhang, and M. Liu, "Subjective and objective quality assessment for images with contrast change," in *IEEE Int. Conf. Image Processing*, 2013, pp. 383–387.

[5] A. Tripathi, S. Mukhopadhyay, and A. Dhara, "Performance metrics for image contrast," in *Int. Conf. Image Information Processing*, 2011, pp. 1–4.

[6] Z. Wang, A. C. Bovik, H. R. Sheikh, and E. P. Simoncelli, "Image quality assessment: From error visibility to structural similarity," *IEEE Trans. Image Process.*, vol. 13, no. 4, pp. 600–612, 2004.

[7] N. Ponomarenko, V. Lukin, A. Zelensky, K. Egiazarian, M. Carli, and F. Battisti, "TID2008-a database for evaluation of full-reference visual quality assessment metrics," *Adv. Modern Radioelectron.*, vol. 10, no. 4, pp. 30–45, 2009.

[8] N. Ponomarenko, O. Ieremeiev, V. Lukin, K. Egiazarian, L. Jin, J. Astola, B. Vozel, K. Chehdi, M. Carli, and F. Battisti *et al.*, "Color image database TID2013: Peculiarities and preliminary results," in *4th Euro. Workshop on Visual Information Processing*, 2013, pp. 106–111.

[9] E. C. Larson and D. Chandler, *Categorical image quality (CSIQ) database*, 2010 [Online]. Available: http://vision.okstate.edu/csiq

[10] Z. Wang, E. P. Simoncelli, and A. C. Bovik, "Multiscale structural similarity for image quality assessment," in *IEEE Asilomar Conf. Signals, Systems and Computers*, 2003, vol. 2, pp. 1398–1402.

[11] Z. Wang and Q. Li, "Information content weighting for perceptual image quality assessment," *IEEE Trans. Image Process.*, vol. 20, no. 5, pp. 1185–1198, 2011.

[12] A. Liu, W. Lin, and M. Narwaria, "Image quality assessment based on gradient similarity," *IEEE Trans. Image Process.*, vol. 21, no. 4, pp. 1500–1512, 2012.

[13] L. Zhang, L. Zhang, X. Mou, and D. Zhang, "FSIM: A feature similarity index for image quality assessment," *IEEE Trans. Image Process.*, vol. 20, no. 8, pp. 2378–2386, 2011.

[14] W. Xue, L. Zhang, X. Mou, and A. C. Bovik, "Gradient magnitude similarity deviation: A highly efficient perceptual image quality index," *IEEE Trans. Image Process.*, vol. 23, no. 2, pp. 684–695, 2014.

[15] L. Zhang, Y. Shen, and H. Li, "VSI: A visual saliency induced index for perceptual image quality assessment," *IEEE Trans. Image Process.*, vol. 23, no. 10, pp. 4270–4281, 2014.

[16] H. R. Sheikh and A. C. Bovik, "Image information and visual quality," *IEEE Trans. Image Process.*, vol. 15, no. 2, pp. 430–444, 2006.

[17] H. R. Sheikh, M. F. Sabir, and A. C. Bovik, "A statistical evaluation of recent full reference image quality assessment algorithms," *IEEE Trans. Image Process.*, vol. 15, no. 11, pp. 3440–3451, 2006.

Authorized licensed use limited to: Access paid by The UC Irvine Libraries. Downloaded on March 24,2021 at 13:49:33 UTC from IEEE Xplore. Restrictions apply.